Polymer 50 (2009) 4571–4576

Contents lists available at ScienceDirect

Polymer

journal homepage: www.elsevier.com/locate/polymer

Molecular and mechanical properties of hydroxypropyl methylcellulose solutions during the sol:gel transition

Gurjit S. Bajwa [a,1], Chris Sammon [c,*], Peter Timmins [b], Colin D. Melia [a]

[a] Formulation Insights, School of Pharmacy, University of Nottingham, NG7 2RD, UK
[b] Biopharmaceutics R&D, Research and Development, Bristol-Myers Squibb, Reeds Lane, Moreton, Merseyside L46 1QW, UK
[c] Materials and Engineering Research Institute, Sheffield Hallam University, Sheffield S1 1WB, UK

ARTICLE INFO

Article history:
Received 6 April 2009
Received in revised form
26 June 2009
Accepted 30 June 2009
Available online 7 July 2009

Keywords:
FTIR-ATR
Thermal gelation
Water

ABSTRACT

This paper outlines the latest findings in our work to understand the fundamental interactions within hydrated hydroxypropyl methylcellulose (HPMC) at elevated temperature. ATR-FTIR spectroscopy was used to relate molecular interactions to the rheological changes in aqueous HPMC solutions during the sol:gel transition. Sol:gel transition temperatures determined using ATR-FTIR spectroscopy, oscillatory rheology and turbidimetry were in agreement to within experimental error. ATR-FTIR spectroscopy provided direct evidence of increased hydrophobic interactions within the gel network through a shift to lower wavenumber of ν_{as}(CH) vibrations observed during the gelation process. In addition, the FTIR spectra provide evidence that the structure of the polymer network is different in the thermo-formed gel, to that which exists in viscous solution. Both the rheological and ATR-FTIR data confirmed the supposition that thermal gelation is a two stage process. The first stage has been attributed to the disruption of native cellulosic bundles and this is supported by the changes in both the storage modulus and intensity of the ν(CO) band at low temperatures. The second stage corresponded to phase separation and gelation resulting from increased hydrophobic interactions between polymer chains at elevated temperatures.

1. Introduction

Cellulose is a linear polysaccharide with an extensive hydrogen bonded, crystalline structure. Its poor aqueous solubility imposes considerable restrictions on its practical applications. Alkyl or hydroxyalkyl substitution of a fraction of the hydroxyl positions results in cellulose ether derivatives in which intermolecular hydrogen bonding is disrupted and water solubility is enhanced [1]. These polymers have widespread applications in construction materials, paints, paper manufacture, textile industry, cosmetics, foods, and pharmaceuticals [2].

Solutions of alkyl cellulose ethers undergo a thermoreversible sol:gel phase transition at elevated temperatures, in which a phase-separated structured gel is formed on heating [3–5]. Kobayashi and co-workers have examined the thermoreversible gelation of methylcellulose (MC) using rheological, small-angle neutron scattering, and dynamic light scattering techniques [5]. They proposed a two stage gelation process in which the first stage was attributed to clustering of hydrophobic groups, whereas the second stage corresponded to phase separation of polymer-rich and polymer-lean regions, accompanied by gelation at elevated temperatures. A similar mechanism has been proposed by Carlsson et al. to explain the gelation of ethyl hydroxyethyl cellulose solutions [6]. They suggested that re-orientation of polymer chains into micelle-like clusters occurs at low temperatures and is followed, at elevated temperatures by the formation of a phase-separated gel network, through interaction between hydrophobic segments of the polymer chains. However, from ^{13}C NMR studies, Ibbett and co-workers have proposed that in the first stage, highly substituted regions of the polymer first separate by forming micelle crosslinks [7]. Further separation then extends and connects these micelles in stage 2, leading eventually to the formation of a porous water-filled network. Haque and co-workers studied the thermoreversible gelation of methylcellulose and hydroxypropyl methylcellulose (HPMC) using oscillatory rheology, differential scanning calorimetry (DSC), light scattering and ^{1}H NMR [3,4]. A two stage gelation process was also proposed. At low temperatures it was suggested that the residual crystallinity causes polymer chains to be dispersed in bundles. During heating, these gradually disintegrate (stage 1) before hydrophobic association of chains leads to gelation (stage 2) at elevated temperatures.

* Corresponding author. Tel.: +44 (0)114 225 3069; fax: +44 (0)114 225 3501.
E-mail address: c.sammon@shu.ac.uk (C. Sammon).
[1] Present address: Material Science and Oral Products Centre of Emphasis, Pharmaceutical R&D, Pfizer, Sandwich, Kent CT13 9NJ, UK.

0032-3861/$ – see front matter © 2009 Elsevier Ltd. All rights reserved.
doi:10.1016/j.polymer.2009.06.075

The mechanisms proposed above, all involve the accumulation of dense hydrophobic aggregates on reaching a critical temperature. In the case of HPMC, the distribution of substituents is heterogeneous as a result of the manufacturing process [1,8], and the heterogeneous distribution of methoxyl moieties appears to be crucial for the thermal gelation process. The extent of methoxyl and hydroxypropyl substitution markedly affects the sol:gel transition temperature [6]. Increasing methoxyl substitution lowers the incipient gelation temperature, whereas increased hydroxypropyl substitution, raises it. The latter effect is explained by the hydroxypropyl groups forming a stable solvate shell in water, but also by the bulkiness of these groups, which sterically hinders intermolecular association [1,9].

Gelation phenomena in non-ionic cellulose ether solutions has been studied by dynamic light scattering [3,5], small-angle neutron scattering [5], microcalorimetry [10,11], rheology [12,3–5], fluorescence [13,14], and NMR [4,15]. Attenuated total reflectance-Fourier transformed infrared (ATR-FTIR) spectroscopy may however, have the potential to provide detailed information *in situ* on a molecular level during the phase transition, particularly with respect to hydrophobic polymer/polymer interactions and polymer/water interactions. ATR-FTIR has also become an important tool for characterising hydrogen bonding in aqueous systems [16–18] and determining the interactions between sorbed water and polymer matrices [19–21]. FTIR has been used to characterise the gel structure of a number of systems including synthetic polymers [22,23], proteins [24,25], and starches [26–29] and been used to study the gelation processes of a number of systems including corn and potato starch [27], waxy-maize starch [29], and wheat starch [26]. FTIR in transmission mode has been used to examine phase changes in potato starch solutions [28], ethyl hydroxyethyl cellulose [30] and we have previously reported the significant and reproducible increase in intensity of the ν(CO) region of aqueous K4M [31] and E4M [32] HPMC solutions subjected to a temperature ramp in a sealed environment.

The aim of this work is to utilise ATR-FTIR spectroscopy to gain further insights into the molecular changes during the thermal gelation process, and to relate these to the rheological changes in aqueous HPMC solutions during the sol:gel transition. The HPMC grade used in this work contained 9.3% hydroxypropyl and 29.5% methoxyl content. Understanding the molecular origin of the gelation mechanism and the way in which this is related to mechanical behaviour can provide important information for the intelligent formulation of foods, cosmetics and pharmaceuticals.

2. Materials and methods

2.1. Materials

HPMC Methocel® E4M CR Premium EP/USP, (batch BN OD16012N32, 9.3% hydroxypropyl, 29.5% methoxyl, The Dow Chemical Company) was a kind gift of Colorcon Ltd, Dartford, UK. Low viscosity silicone oil (100 mPa s) was obtained from Sigma–Aldrich Co Ltd, Dorset, UK. Solutions were prepared in degassed Maxima HPLC grade water (USF Elga, Buckinghamshire, UK) with a maximum conductance of 18.2 MΩcm.

2.2. Preparation of HPMC solutions

Solutions containing 2% and 5% w/w HPMC were prepared by adding HPMC powder to the weight of water required to make up to one tenth of the final weight, with vigorous agitation until the aggregates of powder were visually dispersed, and refrigeration for 24 h at 4 °C to allow polymer hydration. The dispersions were then made up to weight, stirred for 2 h using a bench top magnetic stirrer and stored refrigerated for 72 h prior to use.

2.3. Rheological measurements

Storage (G') and loss (G'') moduli, and tan δ (G''/G') were determined as a function of temperature using a Bohlin C–VOR (Bohlin Instruments Ltd, UK) fitted with 40 mm acrylic parallel plate (PP/40) geometry. A continuous temperature sweep (from 10 to 85 °C and back) was undertaken at a rate of 1 °C min^{-1}, an angular frequency of 0.5 Hz and at 5% strain, which was within the linear viscoelastic region of the polymer solutions. To prevent dehydration of sample during the rheological measurements, a thin layer of low viscosity silicone oil was placed on the peripheral surface of the sample held between the plates.

2.4. ATR-FTIR measurements

ATR-FTIR spectra were collected using a temperature-controlled Golden Gate™ single reflection ATR accessory (SpectraTech) coupled to a ThermoNicolet Nexus FTIR spectrometer. Samples were placed in direct contact with the ATR crystal and sealed using a 'volatiles' cap to ensure no water loss during the heating and cooling cycles. The samples were allowed to equilibrate for 8 min at the required temperature prior to data collection. Data were collected by averaging 64 scans at 4 cm^{-1} resolution. A blank ATR crystal, and 18.2 MΩcm water at the same temperature and under the same conditions were used as reference backgrounds.

2.5. Turbidimetric measurements

Cloud point measurements were made in a temperature-ramped white light turbidimeter in 10 mm pathlength cells (C. Washington, Nottingham, UK). The cloud point temperature (CPT) was determined as the temperature at which light transmission was reduced to 50% [33].

2.6. Peak fitting procedure

The complex ν(CO) band between 1215 and 900 cm^{-1} is associated with the HPMC polymer and is comprised of numerous C–O vibrations; including glycosidic C–O–C, C–OH, C–OCH_3, C–OCH_2-CH_2OH. This band was fitted into its primary peaks (mixed Gaussian (20%)/Lorentzian (80%)) using the peak fitting application on Grams/AI v7.02 (Thermo Galactic, Woburn, USA). Eight peaks were fitted to the ν(CO) band with centres identified at 1215, 1197, 1152, 1119, 1079, 1050, 1025, and 945 cm^{-1}. The infrared spectrum of any cellulose ether compound is complicated and the exact band assignments are difficult. The difficulty arises mainly from the absence of a model polymer with a precise distribution of substituents [34]. Band assignments made in the present work are based on those reported for cellulose and some of its derivatives [31,35,30].

3. Results

Fig. 1a shows how the viscoelastic moduli (G' and G'') and tan δ values of 2% w/w HPMC solutions changed during the heating cycle. The cloud point of this solution (55.9 ± 0.2 °C ($n = 3$)) is also shown on the rheogram. Raising the temperature from 10 °C results in the storage modulus (G') decreasing to approximately 43 °C whereupon G' then increased in a gradual manner through the cloud point (CPT). It has been reported previously that CPT is not always coincident with rheological gelation and may precede or lag behind by a few degrees [36]. The inflexion around 43 °C during the

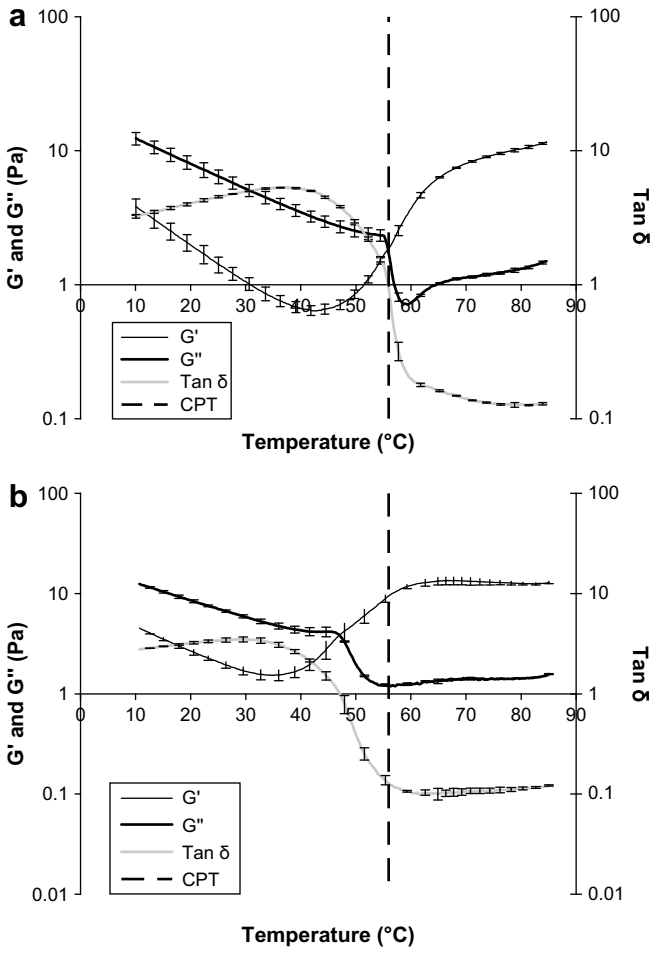

Fig. 1. The effect of temperature on the viscoelastic moduli (G', G'') and tan δ of 2% w/w HPMC solutions during the (a) heating and (b) cooling cycles. Experimental variables; PP/40 geometry, 5% strain, frequency 0.5 Hz, and temperature ramp 1 °C min^{-1}. CPT = Cloud point temperature determined by turbidimetry. Mean values ($n = 3$) ± 1 SD.

heating cycle has been previously reported for both methylcellulose and HPMC solutions. The reduction in G' has been attributed to the progressive disruption of native cellulosic 'bundles', whereas the subsequent increase in G' has been interpreted as arising from the unbundling of the constituent strands of polymer at the ends of the bundles, followed by the formation of a network of swollen clusters [3,4].

The loss modulus (G'') progressively decreased but then dropped sharply at approximately 56 °C. This is a result of high molecular weight fractions of polymer precipitating from solution [11]. At tan $\delta = 1$ the polymer solution exhibited a change from a liquid-like to solid-like system ($G' > G''$), we have used this value (tan $\delta = 1$ at 56 °C) to indicate the start of the gelation process. The gel point defined by this method corresponded with the CPT value.

Tan δ (G''/G') behaviour exhibited four distinct phases during the heating cycle (I) a shallow increase (10–40 °C) resulting from the disruption of cellulosic 'bundles', increasing polymer chain mobility and weakening of polymer:water hydrogen bonding, (II) a decrease (40–56 °C) due to the formation of a tenuous network of swollen clusters that resulted from the 'unbundling' phenomena (increase in volume), (III) a sharp reduction between 56 and 60 °C corresponding to the formation of an coherent elastic gel structure (40–60 °C), and finally (IV) an elastic gel which exhibited little temperature dependence at elevated temperatures (60–85 °C). On cooling, (Fig. 1b) there was significant hysteresis (tan $\delta = 1$ at 46 °C) which, using the Haque and Morris interpretation [3] would indicate that the dissociation of aggregated cellulosic 'bundles' occurs at a higher temperature than when they re-form on cooling.

Previously [32] we have shown that ATR-FTIR can be applied successfully to monitor thermal gelation processes in HPMC solutions. The onset of thermal gelation was shown to be marked by an increase in the intensity of the HPMC band at ~1050 cm^{-1} in the spectrum of the solution. These intensity increases were shown to be accompanied by decreases in the intensity of bands associated with water and this was interpreted as evidence of syneresis. A partial least squares model was used to quantify the decrease in concentration of water within the gel and some of the limitations of this data were discussed. The gel point temperature obtained from the ATR-FTIR data was shown to be in good agreement with that obtained using two separate methods; differential scanning calorimetry and oscillatory rheometry. The changes in the band shape of the ν(OH) band during gelation indicated a preferred removal of weakly hydrogen bonded water species from between the polymer layers during gelation.

Fig. 2a shows the effect of increasing the temperature of an aqueous 2% w/w HPMC solution through the sol:gel transition, measured using ATR-FTIR spectroscopy. From the figure it is clear that the intensity of the complex band between 1200 and 950 cm^{-1} changes as a function of temperature. This band is associated with the HPMC polymer and is comprised of numerous C–O vibrations; including glycosidic C–O–C, C–OH, C–OCH_3, C–OCH_2CH_2OH, we will

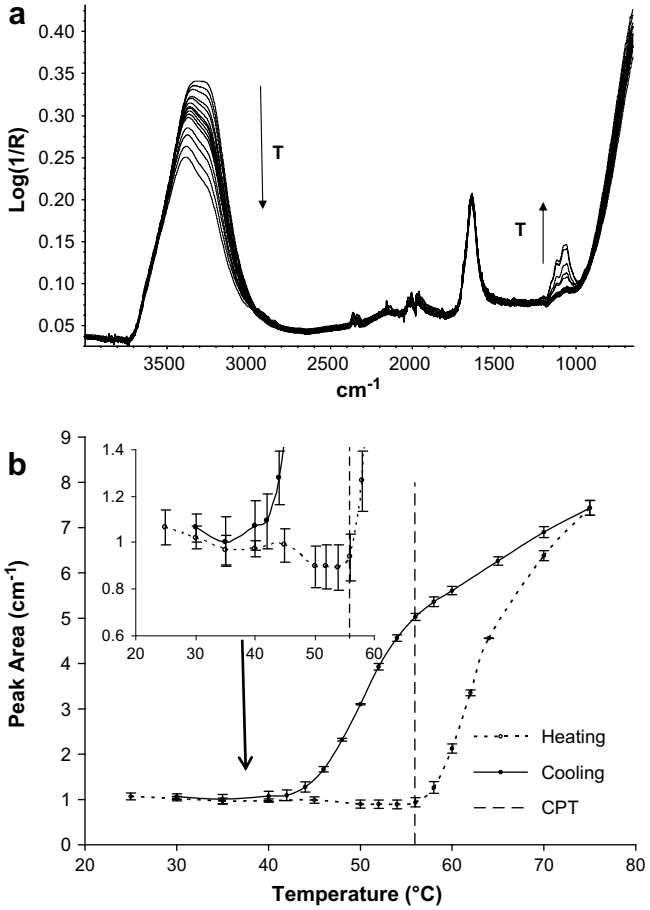

Fig. 2. The effect of temperature on (a) the infrared spectrum of 2% w/w HPMC solution (b) the integrated peak area of the polymer related ν(CO) band. ATR-FTIR spectra collected using the Golden Gate apparatus from averaging 64 scans with a resolution of 4 cm^{-1}. Temperature range 30–75 °C at 5 °C intervals. CPT = Cloud point temperature. (Mean ($n = 3$) ± 1 SD).

refer to this band as the ν(CO) band during this discussion. At temperatures below 45 °C we observe a subtle decrease in the intensity of these bands. This we assume is related to the reduction in density of the HPMC solution and supports the changes observed in the storage modulus (G') at the same temperature. Above around 56 °C (the gelation point) there is a significant increase in the intensity of the ν(CO) band. The implication of this increase in band intensity is that during gelation, the concentration of HPMC within the evanescent field is increasing, which is probably due to the gel layer having a higher density than the HPMC solution (and water) and the geometry of the system means that the gel 'falls' into the evanescent field. Conversely the intensity of infrared bands associated with water (~3500 and 1630 cm^{-1}) decrease within the same temperature range, as has been reported previously for a different grade of HPMC (USP2208, Methocel K4M) [31]. The ν(OH) band of pure liquid water is highly sensitive to temperature, with changes in shape and intensity observed at different temperatures, but the bending mode has been shown to be insensitive to such changes [31,32]. In previous work we have quantified the apparent loss of water at the ATR/polymer solution interface using the intensity of the δ(OH) band as a marker, and used the ν(OH) band to show how the water is somewhat differently organised within the gel network compared to the polymer solution [32]. Here we will try to relate the changes in the water structure with shape changes in the ν(CO) band, the oscillatory rheometry measurements and the perceived understanding of the gelation mechanism of cellulose ether solutions.

The integrated area of the ν(CO) band as a function of temperature is shown in Fig. 2b. There is a clear and distinct increase in intensity as a function of temperature that begins ~56 °C. This is the same temperature at which $\tan\delta = 1$ and the cloud point determined by turbidity measurements and therefore we conclude that these intensity changes are related to the sol:gel transition. In agreement with previous rheology and DSC measurements [32] the cooling curve shows evidence of a hysteresis loop, further supporting the assertion that the source of the intensity changes is related to the gelation process. A closer inspection of the 'pre-gelation' region between 45 and 56 °C (inset graph Fig. 2(b)) suggests a subtle decrease in the overall intensity of the ν(CO) band as the temperature is increased. This observation would concur with the assertions of Haque and co-workers [3,4], that a progressive disruption of native cellulosic 'bundles' results in a volume increase, which in turn would result in a decrease in the concentration of HPMC in the evanescent field.

To investigate if the increase in intensity of the HPMC bands shown in Fig. 2a are simply the result of an increase in the concentration of HPMC at the ATR interface or if there is additional information regarding polymer/water and polymer/polymer interactions it is necessary to compare this data with standard HPMC solutions prepared in the manner described by Banks and co-workers [31]. The ATR-FTIR spectra of 2, 5, 10, 20 and 30% (w/w) HPMC solutions are shown in Fig. 3a. The integrated area of the ν(CO) band plotted against polymer concentration is a straight line (Fig. 3b), indicating there are no gross modifications to the ε of all of the HPMC bands as a function of concentration. One perhaps might anticipate some changes to the shape of the complex ν(CO) band as a function of polymer concentration as the numbers and types of interactions (hydrogen bonding/hydrophobic attractive forces) are likely to change given the amphiphilic nature of the cellulose ether.

Fig. 4a and b were generated using the intensity of the 1390 cm^{-1} band for normalisation purposes, and aid the analysis of the subtle changes that occur in the band shape. A comparison of the normalised peak shape of HPMC in powder form and in aqueous solutions at 5%, 10%, 20% and 30% w/w concentrations is provided in Fig. 4a. There are several points that should be noted

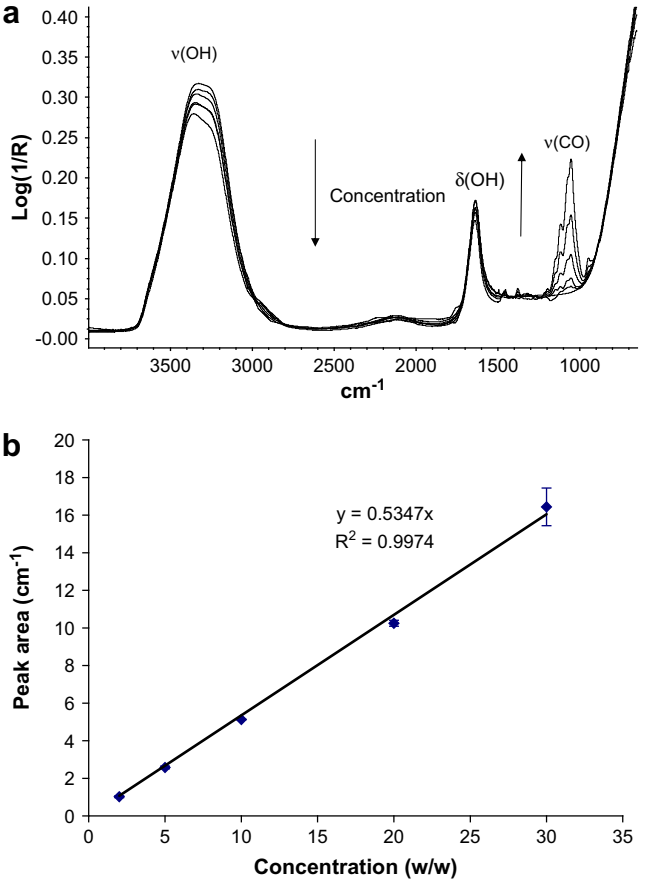

Fig. 3. (a) Effect of polymer concentration (2, 5, 10, 20, 30% w/w) on the infrared spectrum of aqueous HPMC at 30 °C. (b) Relationship between polymer concentration and the integrated peak area of the polymer related ν(CO) peak ATR-FTIR spectra collected using the Golden Gate apparatus from averaging 64 scans with a resolution of 4 cm^{-1}. (Mean ($n = 3$) ± 1 SD).

from this figure. Firstly, there is a very dramatic change in the shape of the complex series of bands between 1200 and 950 cm^{-1} (subsequently referred to as the ν(CO) band) the shapes of the solution spectra and the dry powder are compared, this we attribute to the differences in the nature of hydrogen bonding in these systems. In the solution state, intermolecular hydrogen bonding between water and the polymer backbone will dominate, whereas a range of interactions will occur in the solid state including sorbed water/polymer interactions and inter- and intra-molecular polymer/polymer interactions [31]. The most obvious change is the reduction in intensity of the ~1025 cm^{-1} peak in the solution, but there is also an interesting but more subtle change in the band assigned to the O-Me vibrations ~1200 cm^{-1}. This is a single band in the 'dry' state and a doublet in the solution state. This may be an indication of attractive methyl/methyl interactions and it could potentially enable us to distinguish between methyl groups that are interacting with near neighbours, and those which are not.

As the concentration of HPMC increases there is a subtle change in the shape of the ν(CO) band. The intensities of peaks ~1152, 1119 and 1079 cm^{-1} vary nonlinearly in comparison with the peaks ~1025 and 1052 cm^{-1}. The implication is that functional groups associated with these bands are subjected to a subtly different environment as the solution concentration of the polymer is increased, leading to perturbation of the extinction coefficient (ε) of these vibrational bands and changes in intensity. Studies of the influence of water concentration, on the band intensity of functional groups that strongly hydrogen bond, indicate that perturbations in

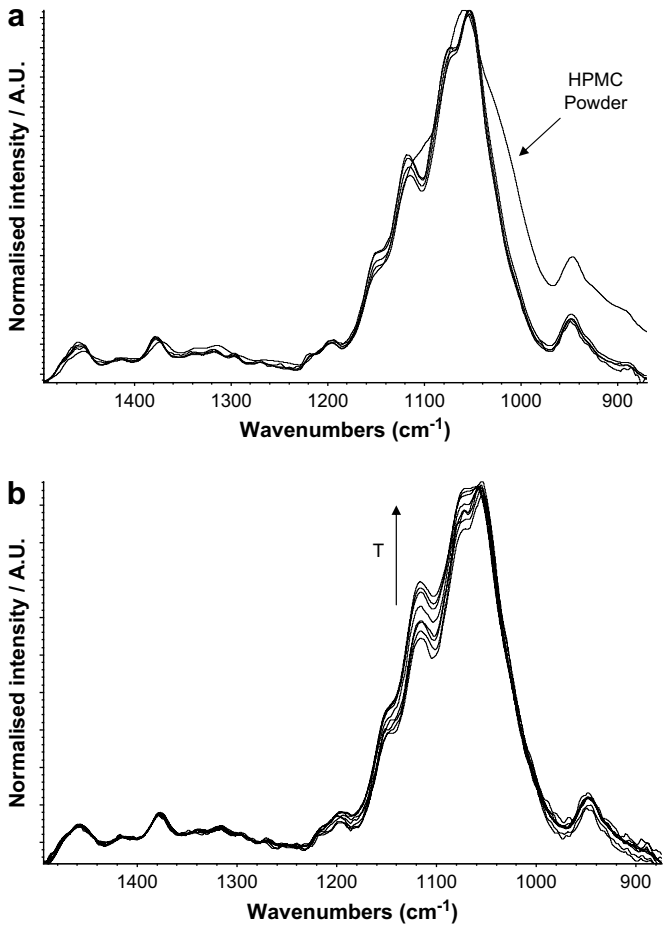

Fig. 4. (a) Normalised spectra of HPMC powder and 5%, 10%, 20% and 30% w/w HPMC solutions at 30 °C. (b) Normalised spectra of 5% w/w HPMC solution as a function of temperature. Spectra were normalised using the intensity of the 1390 cm^{-1} band. Temperature range 30–75 °C at 5 °C intervals.

intensity do occur whilst they are involved in hydrogen bonding. In the late 1980's, Ford's group [37–41] conducted a systematic study into the effects of hydrogen bonding on the infrared band intensities of the carbonyl bands of ketones and found intensity increases in hydrogen bonded species compared with non-hydrogen bonded species. Therefore one explanation for the relative intensity changes observed in Fig. 4a, is that the amount of intermolecular hydrogen bonding between polymer chains and the solvent water may be different at different concentrations. Calculations based on the statistical average molecular weight of each monomer unit, indicate that there are over 400 water molecules per repeat monomer unit for a 5% HPMC solution and only ~50 for a 30% HPMC solution.

Fig. 4b shows the ν(CO) band shape changes during gelation. These are clearly different to those shown in Fig. 4a where the only variable is HPMC concentration. The obvious implication for this observation is that the 'structure' of the polymer (in terms of the local environment 'experienced' by the polymer chains) within the gel is different to the polymer structure in the viscous solutions. Bands ~1079, 1119 and 1152 cm^{-1} respond similarly as a function of concentration and gel formation, whereas bands ~1052 and 1025 cm^{-1} respond differently. Fig. 5 shows this more clearly. In this plot, band area ratios obtained using a curve fitting routine, are plotted as a function of temperature for the 1079/1119 cm^{-1} and the 1079/1025 cm^{-1} bands. At the temperature of gelation, the 1079/1025 cm^{-1} band ratio changes because the 1025 cm^{-1} band becomes relatively weaker. Paul and Ford [37–41] have shown that

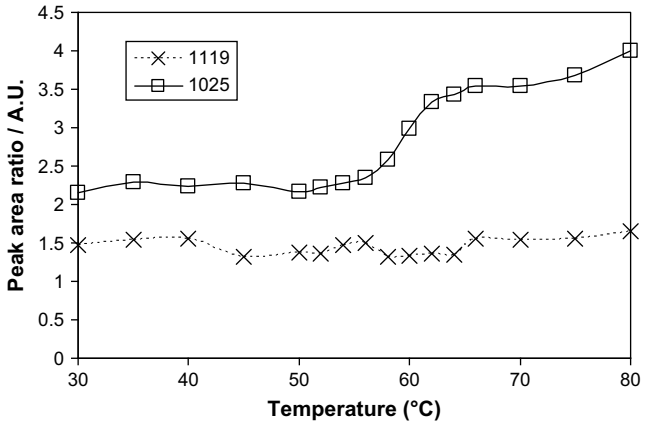

Fig. 5. The band area ratios for 1079/1119 cm^{-1} and 1079/1025 cm^{-1} bands of 5% w/w HPMC solutions as a function of temperature.

changes in the electrostatic interactions within a system (such as hydrogen bonding) can significantly influence the intensity bands associated with polar groups. In this instance, a decrease in the relative intensity of these bands would indicate a reduction in the average number of hydrogen bonds between the polymer backbone and the water media. This is supported by the observed reduction in the intensity of the δ(OH) over the same temperature range (evidence of syneresis). Based on these findings, it seems most probable that the 1052 and 1025 cm^{-1} bands are associated with alcoholic ν(C–O) vibrations.

It seems logical that if the numbers of water/polymer interactions decrease as a result of phase separation and syneresis, then polymer/polymer interactions should be seen to increase in numbers or strength. It has been shown that for NIPAM and PEO–PPO–PEO based systems, that attractive forces between methyl groups result in a shift to lower wavenumbers of the antisymmetric methyl stretch vibrations during thermal gelation [42,23]. Fig. 6 shows the spectral region between 2980 and 2800 cm^{-1} for 5% w/w HPMC solutions. This is associated with a number of bands related to ν_{as}(CH) vibrations of the HPMC system. These bands are fairly broad indicating that they vary in species and/or environment but as HPMC is a heterogeneous material, this is expected. The ν_{as}(CH) bands were shown to shift to lower wavenumber by ~6 cm^{-1} during the sol–gel transition, as a result of increased attractive forces between non-polar/non-polar groups along the cellulose backbone. This is the first direct evidence of such interactions in

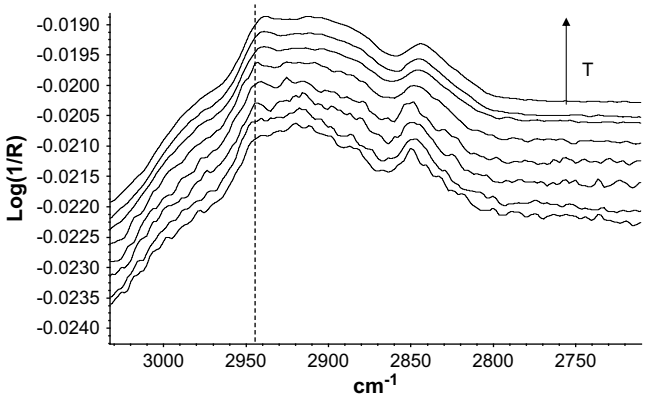

Fig. 6. Spectra of ν_{as}(CH) bands of 5% w/w HPMC solutions as a function of temperature (30–75 °C at 5 °C intervals). ATR-FTIR spectra collected using the Golden Gate apparatus from averaging 64 scans with a resolution of 4 cm^{-1}.

aqueous HPMC systems and clearly points to these interactions being heavily involved in the gelation mechanism.

Detailed analysis of the ATR-FTIR spectra of 5% HPMC solutions over the temperature range 30–80 °C can therefore be summarised as follows:

1. As the temperature of the system is increased and the solution forms an opaque gel, there is a significant increase in intensity of the bands between 1200 and 900 cm^{-1} which are generally associated with ν(C–O) and ν(C–C) bands of the HPMC polymer.
2. In the heating run, prior to the onset of gelation and precipitation, at temperatures between ~45 and 56 °C (inset graph Fig. 2(b)) there is a decrease in the overall intensity of the bands associated with the polymer, indicating that the concentration of HPMC in the evanescent field is decreasing which is most likely the result of the solution density decreasing.
3. Above the gel point, as the intensity of the 'polymer' bands increase, the intensity of 'water' bands (3600–3000 and ~1630 cm^{-1}) decrease in intensity. This can be interpreted as evidence of syneresis.
4. Close examination of the band shape of the 'polymer' bands shows that there are differences in the shape of the band as it becomes more intense as a function of time. These changes are different to those observed when HPMC concentration is increased at ambient temperatures giving rise to similar intensity changes.
5. Bands ~1052 and 1025 cm^{-1} are shown to have a lower relative intensity than bands ~1079, 1119 and 1152 cm^{-1} and this can be interpreted as a reduction in the amount of polymer/water hydrogen bonding in the system.
6. The ν_{as}(CH) vibrations show a shift to lower wavenumber during gelation which we interpret to mean an increase in the numbers of attractive 'hydrophobic' interactions between the polymer backbone.

4. Conclusion

ATR-FTIR spectroscopy has been applied successfully to monitor the gelation process of HPMC solutions at elevated temperatures. The sol:gel transition temperature determined using ATR-FTIR spectroscopy, oscillatory rheology and the turbidimetric measurement of cloud point temperature appear to be in good agreement within experimental error. To the best of our knowledge the results from the ATR-FTIR spectroscopy study have for the first time provided direct evidence of increased hydrophobic interactions. (ν_{as}(CH) vibrations show a shift to lower wavenumber) during the gelation process. In addition the FTIR spectra provide evidence that the structure of the polymer network, (in terms of the local environment experienced by polymer molecules) is different within the gel formed on increasing temperature, to that of the polymer structure that exists in the viscous solution.

The gelation of HPMC proceeded in two stages, as noted by previous workers. The first stage, attributed to the disruption of cellulosic bundles, was supported by the changes in both the storage modulus and intensity of the ν(CO) band at low temperatures. The second stage corresponded to phase separation, accompanied by gelation resulting from increased hydrophobic interactions at elevated temperatures.

References

[1] Donges R. British Polymer Journal 1990;23(4):315–26.
[2] Clasen C, Kulicke WM. Progress in Polymer Science 2001;26(9):1839–919.
[3] Haque A, Morris ER. Carbohydrate Polymers 1993;22:161–73.
[4] Haque A, Richardson RK, Morris ER, Gidley MJ, Caswell DC. Carbohydrate Polymers 1993;22:175–86.
[5] Kobayashi K, Huang C, Lodge T. Macromolecules 1999;32(21):7070–7.
[6] Carlsson A, Karlstrom G, Lindman B. Colloids and Surfaces 1990;47:147–65.
[7] Ibbett RN, Philp K, Price DM. Polymer 1992;33(19):4087–95.
[8] Grover JA. In: BeMillier JN, editor. Industrial gums-polysaccharides and their derivatives. 3rd ed. San Diego: Academic Press, Inc.; 1993. p. 475–504.
[9] Hussain S, Keary C, Craig DQM. Polymer 2002;43(21):5623–8.
[10] Li L. Macromolecules 2002;35(15):5990–8.
[11] Sarkar N, Walker LC. Carbohydrate Polymers 1995;27(3):177–85.
[12] Desbrieres J, Hirrien M, Ross-Murphy SB. Polymer 2000;41(7):2451–61.
[13] Nilsson S. Macromolecules 1995;28(23):7837–44.
[14] Ridell A, Evertsson H, Nilsson S, Sundelof LO. Journal of Pharmaceutical Sciences 1999;88(11):1175–81.
[15] Weng LH, Zhang LN, Ruan D, Shi LH, Xu J. Langmuir 2004;20(6):2086–93.
[16] Bertie J, Lan Z. Applied Spectroscopy 1995;49(6):840–51.
[17] Max JJ, Chapados C. Applied Spectroscopy 1999;53(12):1601–9.
[18] Max JJ, de Blois S, Veilleux A, Chapados C. Canadian Journal of Chemistry 2001;79:13–21.
[19] Hare DE, Sorensen CM. Journal of Chemical Physics 1992;96(1):13–22.
[20] Libnau FO, Christy AA, Kvalheim OM. Applied Spectroscopy 1995;49(10):1431–7.
[21] Libnau FO, Kvalheim OM, Christy AA, Toft J. Vibrational Spectroscopy 1994;7(3):243–54.
[22] Malik S, Nandi AK. Journal of Physical Chemistry B 2004;108(2):597–604.
[23] Su YL, Liu HZ, Guo C, Wang J. Molecular Simulations 2003;29(12):803–8.
[24] Goeden-Wood NL, Keasling JD, Muller SJ. Macromolecules 2003;36(8):2932–8.
[25] Gosal WS, Clark AH, Pudney PDA, Ross-Murphy SB. Langmuir 2002;18(19):7174–81.
[26] Bulkin BJ, Kwak Y, Dea ICM. Carbohydrate Research 1987;160:95–112.
[27] Iizuka K, Aishima T. Journal of Food Science 1999;64(4):653–8.
[28] Liu Q, Charlet G, Yelle S, Arul J. Food Research International 2002;35(4):397–407.
[29] Wilson RH, Kalichevsky MT, Ring SG, Belton PS. Carbohydrate Research 1987;166(1):162–5.
[30] Ostrovskii D, Kjoniksen AL, Nystrom B, Torell LM. Macromolecules 1999;32(5):1534–40.
[31] Banks SR, Sammon C, Melia CD, Timmins P. Applied Spectroscopy 2005;59(4):452–9.
[32] Sammon C, Bajwa G, Timmins P, Melia CD. Polymer 2006;47(2):577–84.
[33] Sarkar N. Journal of Applied Polymer Science 1979;24:1073–87.
[34] Hirrien M, Chevillard C, Desbrieres J, Axelos MAV, Rinaudo M. Polymer 1998;39(25):6251–9.
[35] Langkilde FW, Svantesson A. Journal of Pharmaceutical and Biomedical Analysis 1995;13(4):409–14.
[36] Chi LL, Martini A, Ford JL, Roberts M. Journal of Pharmacy and Pharmacology 2005;57:533–46.
[37] Paul S, Ford T. Journal of Molecular Structure 1987;160(1–2):67.
[38] Paul S, Ford T. Journal of Molecular Structure 1989;198:65–75.
[39] Paul S, Ford T. Journal of the Chemical Society-Faraday Transactions 2 1981;77:33–46.
[40] Paul S, Ford T. Spectrochimica Acta Part A: Molecular and Biomolecular Spectroscopy 1988;44(6):587–600.
[41] Tshehla T, Ford T, Afr S. Journal of Chemistry 1995;48(3–4):127.
[42] Maeda Y, Nakamura T, Ikeda I. Macromolecules 2001;34:1391–9.